Electronic Supplementary Information

CO_2 reduction on the Li-Ga liquid metal surface

Linlin Ye,[a] Nitu Syed,[b] Dingqi Wang,[a] Billy J. Murdoch,[c] Karma Zuraqi,[c] Masood S. Alivand,[ad] Penny Xiao,[a] Ranjeet Singh,[a] Lianhai Zu,[a] Kathryn A. Mumford,[a] Amanda V. Ellis,[a] Chris F. McConville,[e] Gang Kevin Li,*[a] and Ali Zavabeti *[a□□□□□□□□□□□][c□□□□□□□□□□□]

[a] Department of Chemical Engineering, The University of Melbourne, Parkville, VIC 3010, Australia

[b] School of Physics, The University of Melbourne, Parkville, VIC 3010, Australia

[c] School of Science, RMIT University, Melbourne, Victoria 3001, Australia

[d] Department of Chemical Engineering, Monash University, Clayton, Victoria 3800, Australia

[e] Institute for Frontier Materials, Deakin University, Waurn Ponds, Geelong, Victoria 3216, Australia

* Corresponding authors: li.g@unimelb.edu.au and ali.zavabeti@unimelb.edu.au

Fig. S1 Surface change with time of 0.2 wt. % Li-Ga alloy reacting with CO_2 in a syringe reactor.

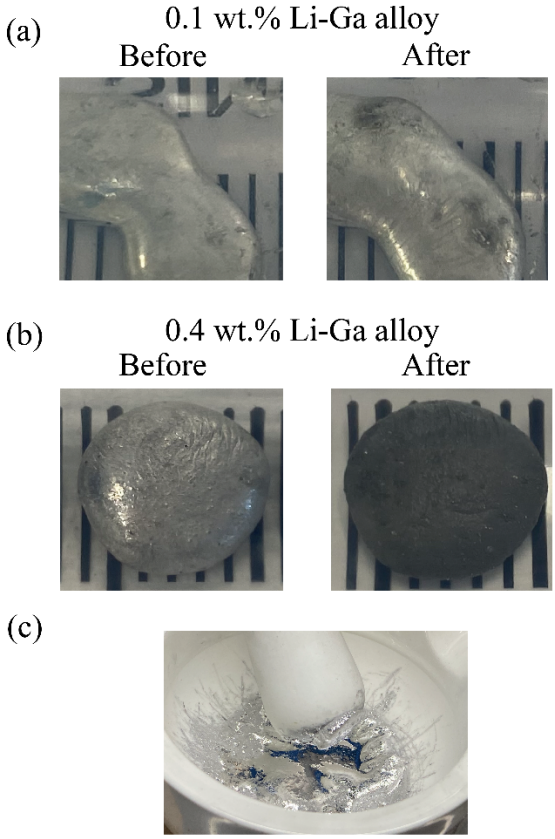

Figure S2. Li-Ga liquid metal alloys with different Li weight percentages. a) 0.1 wt.% showing localized reaction on the surface, b) 0.4 wt.%, c) Paste-like fluidity after the alloying process is seen for 0.4 wt.% alloy.

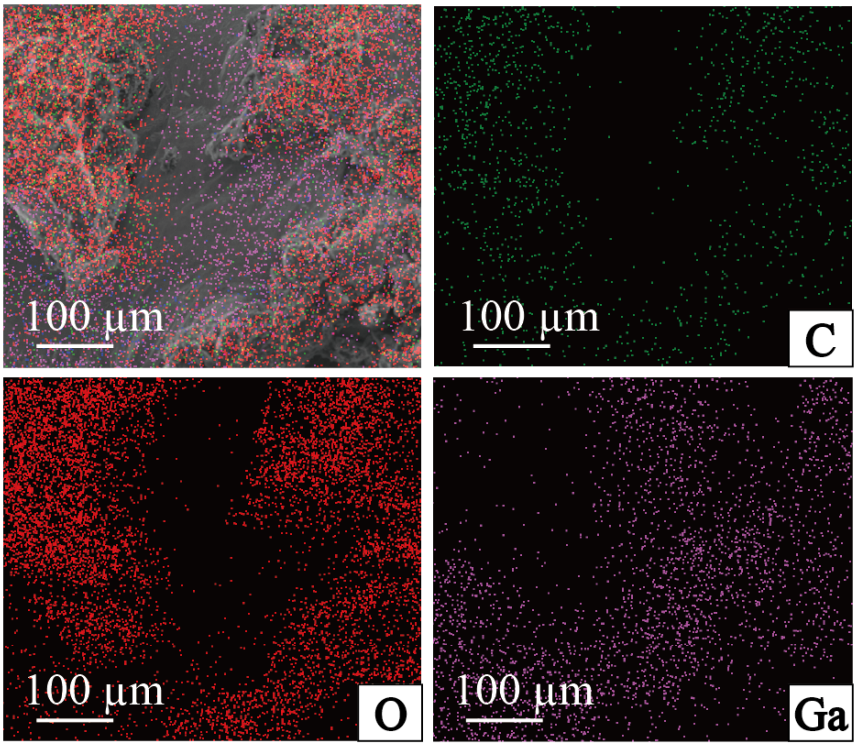

Fig. S3 Elemental mapping on the surface of Li-Ga alloy after reaction showing the gallium base below the crust layer.

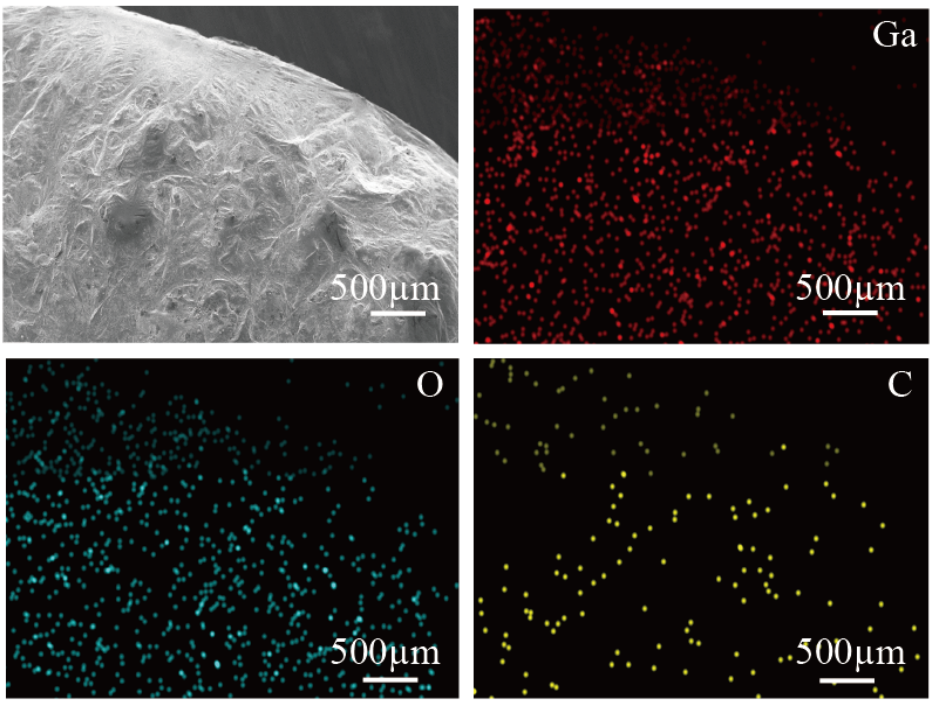

Fig. S4 Elemental mapping on the surface of Li-Ga alloy after reaction with CO_2 at 0 ℃ for one day.

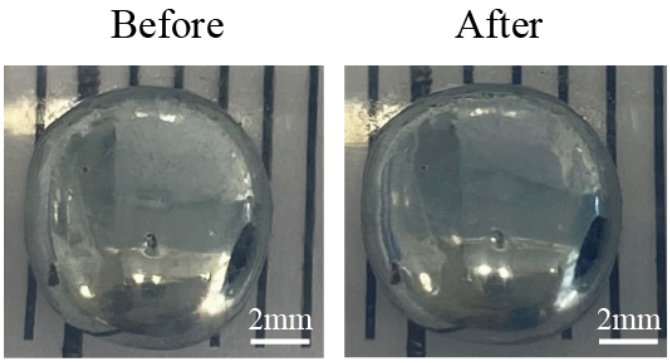

Fig. S5 Li-Ga alloy in an argon atmosphere at 50 ℃ for one day.

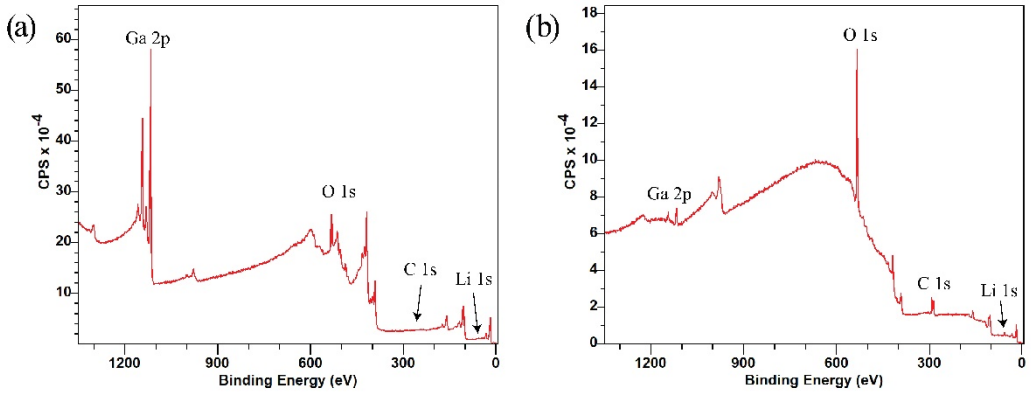

Fig. S6 XPS survey spectra on the surface of liquid metal alloy a) after cleaning the surface with a GCIS ion gun showing no carbon contamination and a low amount of Li is present as shown in bar charts of Fig 1. b) The sample is immediately transferred inside XPS from the analysis chamber into the gas reaction chamber using the transfer arms. After melting and exposing the alloy inside the reaction chamber, the sample was transferred back to analysis chamber using the built-in transfer arm, in which spectra showed awing 40 % increase in signal intensity for Li and peaks corresponding to carbon and carbonate appeared as shown in Fig 3 a-d.

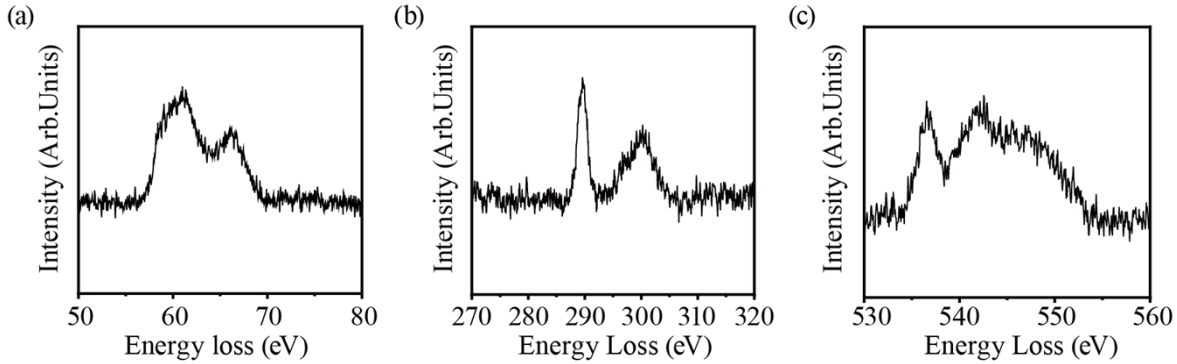

Fig. S7 EELS confirmation of Li_2CO_3[1, 2]. a) The Li K-edge spectrum of Li_2CO_3 b) The C K-edge spectrum of Li_2CO_3. c) The O K-edge spectrum of Li_2CO_3.

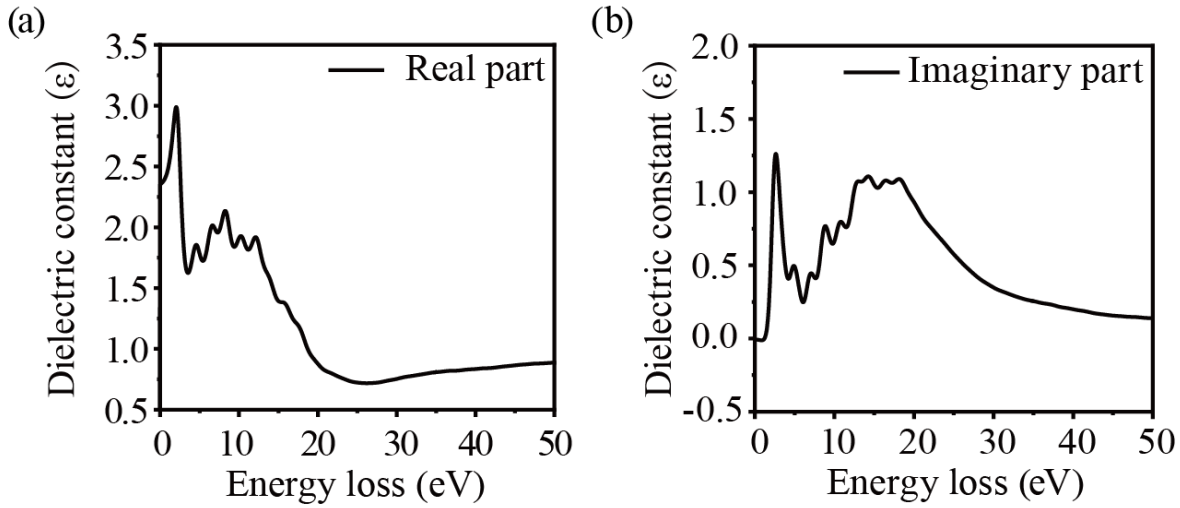

Fig. S8 The a) real and d) imaginary parts of the dielectric constant obtained from EELS.

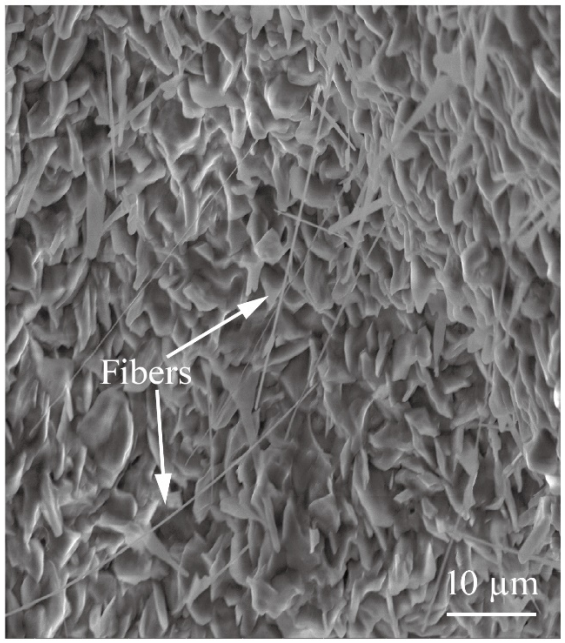

Fig. S9 SEM original image of Figure 3h.

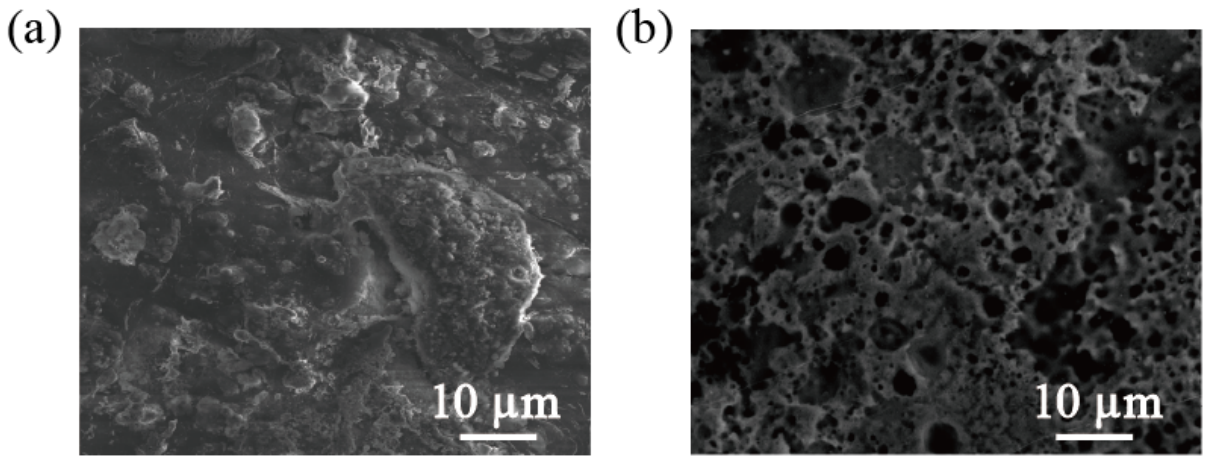

Fig. S10 SEM images for the Li-Ga alloy surface after reaction with CO_2. a) Reactions conducted at a) 50 ℃ and b) 200 ℃ showing the absence of fiber-like structures.

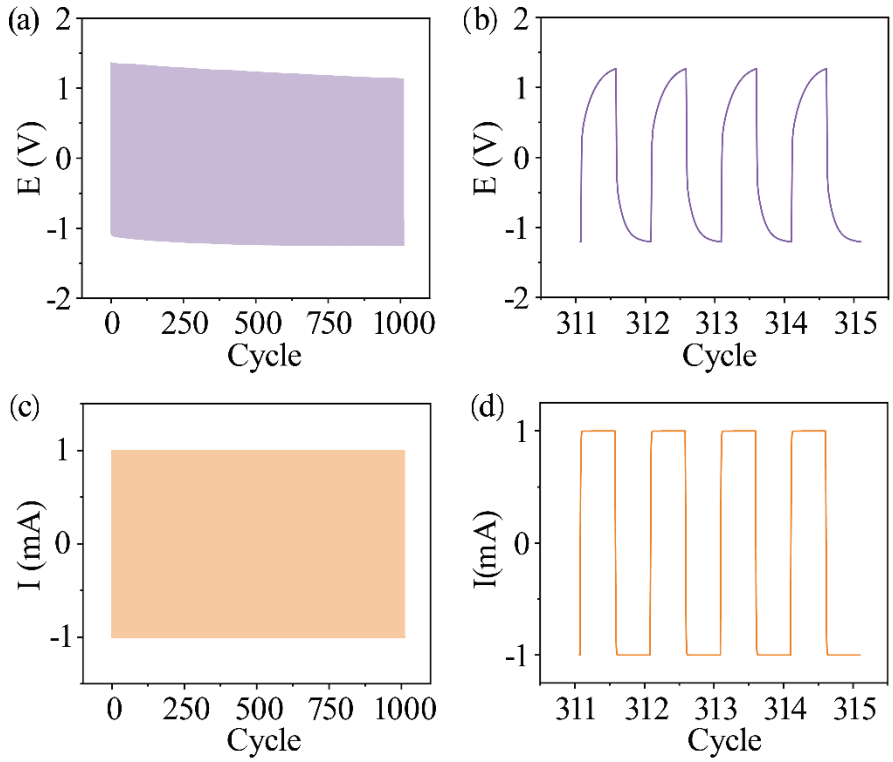

Figure S10. a and c) The charge–discharge cycling tests of the supercapacitor electrodes over 1000 cycles b) and d) are selected cycles for a) and c), respectively. The voltage shown is with respect to open circuit potential.

Table S1. CO_2 consumption in various reaction temperatures

Temperature (°C)	Mass of alloy (mg)	Li (mg)	Li (mmol)	CO_2 consumption (mmol)	CO_2 consumption (mg)	C production (mg)
50	1000	2	0.29	0.17	7.45	1.02
200	1000	2	0.29	0.18	8.06	1.10
500	1000	2	0.29	0.20	8.89	1.21

Table S2 Capacitance of carbon-based electrodes in non-aqueous solvents

Nonaqueous electrolyte	**Electrode**	**C(Fg^{-1})**
$MeEt_3NBF_4$/PC	Wheat straw-based activated carbon	160[3]
[EMIM][BF_4]	Biomass-derived activated porous carbon	80[4]
$TEABF_4$/PC	Carbon nanotubes	158[5]
$CuCl_2$/$EMImBF_4$	Activated carbon	225[5]
EMImBr/$EMImBF_4$	Activated carbon fiber cloths	59[5]
HQ/$Et_3NHTFSI$	Activated charcoal	72[5]
EMIm-BF_4/CAN	Fibrous carbide-derived carbon	105.6[6]
$TBAPF_6$/NMP	Carbon, lithium carbonate and oxide	165*

*This work

Supplementary Information Video 1

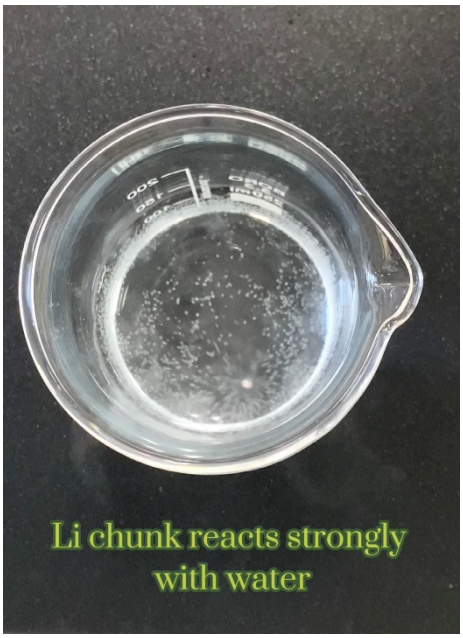

Video S1. Li reacts strongly with water. Lithium is highly reactive and flammable and it reacts rapidly with water at room temperature.

Supplementary Information Video 2

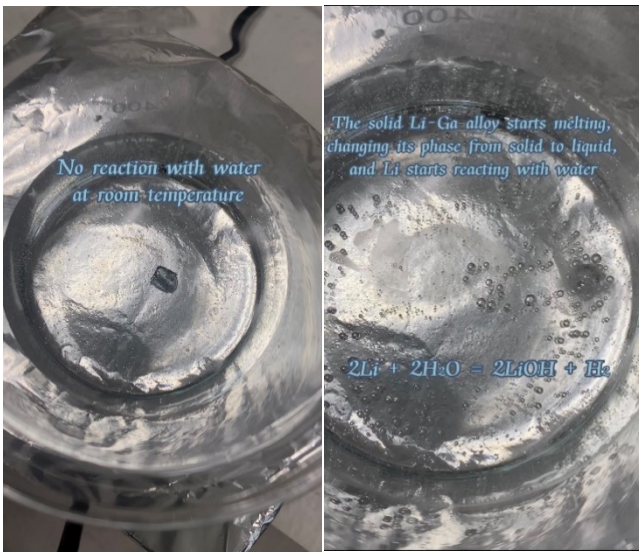

Video S2. On-demand reaction. When the temperature is below the melting point of Li-Ga alloy, the alloy is in its solid state and Li inside Ga would not react with water. When the temperature is above the melting point of the alloy, it becomes liquid and Li starts to react with water, which makes the reaction controllable.

Supplementary Information Video 3

Video S3. High yield of reaction. During the reaction, Li-ions diffuse to the surface and completely react. After reaction, the surface of alloy was covered by a layer of black crust. The crust could be separated easily from the gallium base. When the remaining alloy was dropped into water, there was no reaction with water, showing all the Li migrated to the surface to react with CO_2, no Li left in the gallium base.

References

1. S. Basak, J. Jansen, Y. Kabiri and H. W. Zandbergen, *Ultramicroscopy*, 2018, **188**, 52-58.
2. B. Han, Z. Zhang, Y. C. Zou, K. Xu, G. Y. Xu, H. Wang, H. Meng, Y. H. Deng, J. Li and M. Gu, *Adv Mater*, 2021, **33**.
3. X. L. Li, C. L. Han, X. Y. Chen and C. W. Shi, *Micropor Mesopor Mat*, 2010, **131**, 303-309.
4. N. Sudhan, K. Subramani, M. Karnan, N. Ilayaraja and M. Sathish, *Energ Fuel*, 2017, **31**, 977-985.
5. J. Park, Y. E. Yoo, L. Q. Mai and W. Kim, *Acs Sustain Chem Eng*, 2019, **7**, 7728-7735.
6. S. Malmberg, M. Arulepp, E. Tarasova, V. Vassiljeva, I. Krasnou and A. Krumme, *C-J Carbon Res*, 2020, **6**.